Colocalization of α-actinin and Synaptopodin in the Pyramidal Cell Axon Initial Segment

Diana Sánchez-Ponce , Lidia Blázquez-Llorca , Javier DeFelipe , Juan José Garrido and Alberto Muñoz

The cisternal organelle that resides in the axon initial segment (AIS) of neocortical and hippocampal pyramidal cells is thought to be involved in regulating the Ca^{2+} available to maintain AIS scaffolding proteins, thereby preserving normal AIS structure and function. Through immunocytochemistry and correlative light and electron microscopy, we show here that the actin-binding protein α-actinin is present in the typical cistenal organelle of rodent pyramidal neurons as well as in a large structure in the AIS of a subpopulation of layer V pyramidal cells that we have called the "giant saccular organelle." Indeed, this localization of α-actinin in the AIS is dependent on the integrity of the actin cytoskeleton. Moreover, in the cisternal organelle of cultured hippocampal neurons, α-actinin colocalizes extensively with synaptopodin, a protein that interacts with both actin and α-actinin, and they appear concomitantly during the development of these neurons. Together, these results indicate that α-actinin and the actin cytoskeleton are important components of the cisternal organelle that are probably required to stabilize the AIS.

Keywords: actin cytoskeleton, axon initial segment, calcium, cisternal organelle, synaptopodin

Introduction

The axon initial segment (AIS) is considered to be the site where action potentials are generated, particularly due to the local concentration of voltage-gated ion channels in this region (Stuart et al. 1997; Garrido et al. 2003; Inda et al. 2006; Kole et al. 2008; Yu et al. 2008; Rasband 2010). The integrity of the actin and microtubule cytoskeleton in the AIS is necessary to preserve its normal structure and function (Winckler et al. 1999; Tapia et al. 2010), and this is at least partially reflected by the ability to regulate local Ca^{2+} levels. Indeed, Ca^{2+}-mediated proteolysis of the AIS cytoskeleton produces a dispersion of Na^{+} channels (Schafer et al. 2009), and Ca^{2+}-mediated activity-dependent plasticity leads to the topographic redistribution of Na^{+} channels within the AIS (Kuba et al. 2010; Grubb and Burrone 2010a). The cisternal organelle consists of stacks of membranous cisternae derived from the smooth endoplasmic reticulum, the outermost of which are attached to the axonal plasma membrane (Palay et al. 1968; Peters et al. 1968; Jones and Powell 1969; Sloper and Powell 1979; Kosaka 1980; Somogyi et al. 1983; Benedeczky et al. 1994; Jedlicka et al. 2008). In neocortical and hippocampal cells, the cisternal organelle is thought to provide the AIS with the ability to regulate changes in cytosolic Ca^{2+} concentrations (Bas Orth et al. 2007; Sánchez-Ponce, et al. 2011b), likely including the transient elevations of AIS Ca^{2+} concomitant with action potential generation (Yu et al. 2008, 2010; Bender and Trussell 2009). The expression of the SERCA-type Ca^{2+} pump (Benedeczky et al. 1994), the inositol 1,4,5-trisphosphate (IP_3) receptor Ca^{2+} channel (IP_3R), and the calcium-binding protein annexin 6 (Yamatani et al. 2010; Sánchez-Ponce et al., 2011b) in this structure provides further evidence that the cisternal organelle is involved in regulating Ca^{2+}.

Ankyrin G and the actin cytoskeleton are important elements that maintain the integrity of the cisternal organelle in cultured hippocampal cells, as actin-depolymerizing agents affect its stability in the AIS. In addition, the protein synaptopodin is required to recruit the cisternal organelle to the AIS of neocortical and hippocampal cells (Bas Orth et al. 2007). Synaptopodin is an actin interacting regulatory protein with multiple binding sites for the ubiquitously expressed protein α-actinin (Mundel et al. 1997; Asanuma et al. 2005; Kremerskothen et al. 2005; Faul et al. 2007; Okubo-Suzuki et al. 2008). α-actinin belongs to a family of actin-binding proteins that cross-link and bundle actin filaments (Otey and Carpen 2004), which includes spectrins, dystrophin, and utrophin (Blanchard et al. 1989; Pascual et al. 1997; Asanuma et al. 2005). Accordingly, α-actinin is involved in the organization of the submembranous cortical cytoskeleton where it induces the formation of isotropic networks of short-branched bundles of actin filaments (Wachsstock et al. 1993; Pelletier et al. 2003). However, synaptopodin may regulate the actin-bundling activity of α-actinin by altering its affinity for actin, inducing the formation of long-unbranched parallel bundles of filaments (Asanuma et al. 2005).

Synaptopodin and α-actinin generally colocalize in the hippocampus (Asanuma et al. 2005), and both α-actinin (Capani et al. 2001) and synaptopodin are found in dendritic spines including the spine apparatus. In these structures, synaptopodin is required for the formation and dynamic reorganization of the actin cytoskeleton, and it serves a role in shaping spines and/or linking the actin cytoskeleton with synaptic membrane proteins (Vlachos et al. 2009). In the AIS, synaptopodin has been found in the cisternal organelle (Bas Orth et al. 2007; Sánchez-Ponce et al. 2011b), and while it remains unclear whether α-actinin is associated to the cisternal organelle in the AIS, it is present in the axon hillock at the base of pyramidal cells (Wyszynski et al. 1997; Di Biase et al. 2008). Here, we used immunocytochemistry and confocal and electron microscopy to define the distribution α-actinin in the AIS of different populations of mouse and rat neocortical and hippocampal pyramidal neurons. In addition, we analyzed the appearance of α-actinin immunoreactivity during the development of the AIS, and its colocalization with synaptopodin and actin filaments in cultured hippocampal cells. Finally, we studied the

redistribution of α-actinin and synaptopodin in the cisternal organelle following actin depolymerization by cytochalasin D. These results indicate that along with synaptopodin, α-actinin is an important component of the AIS that may contribute to the stabilization of membranous structures, including the cisternal organelle, the morphological features of which are highly dependent on actin microfilaments.

Materials and Methods

Brain Tissue

C57BL/6 mice (n = 8 males, aged between 30 and 32 days) and Wistar rats (n = 5 males, aged 30 days) were sacrificed by a lethal intraperitoneal injection of sodium pentobarbital, and they were then perfused intracardially with a saline solution followed by 4% paraformaldehyde in 0.1 M phosphate buffer (PB, pH 7.4). All experiments were performed in accordance with the guidelines established by the European Union regarding the use and care of laboratory animals (86/609/EEC). The brain of each animal was removed, postfixed by immersion in the same fixative for 24 h at 4 °C, and serial coronal sections (50-μm thick) were obtained with the aid of a Vibratome (St Louis, MO). The sections were then processed for immunocytochemical staining, and some adjacent sections to those used for immunocytochemistry were Nissl stained.

For immunofluorescence staining, the sections were first rinsed in PB and preincubated for 1 h at room temperature in a stock solution containing 3% normal serum of the species in which the secondary antibodies were raised (Vector Laboratories, Burlingame, CA) diluted in PB with Triton X-100 (0.25%). Thereafter, the sections were incubated for 48 h at 4 °C in the same stock solution containing the following primary antibodies alone or in combination: mouse anti-α actinin (1:500, Sigma A7811, St Louis, MO), mouse anti-synaptopodin (1:100, Acris MAB4919, Herford, Germany), mouse anti-ankyrin G (1:100, Neuromab 75146, Davis, CA), and rabbit anti-synaptopodin (1:250, Sigma S9442). After rinsing in PB, the sections were incubated for 2 h at room temperature in the appropriate combinations of Alexa 488- or Alexa 594-conjugated goat anti-mouse or goat anti-rabbit antibodies (1:2000; Molecular Probes, Eugene, OR). In some sections, actin filaments were stained with Alexa 488 phalloindin in combination with Alexa 594 α-actinin immunostaining. Finally, the sections were washed in PB, mounted in antifade mounting medium (Invitrogen/Molecular Probes) and studied by confocal microscopy (Zeiss, 710). Z sections were recorded at 0.2- to 1-μm interval through separate channels and subsequently; ZEN 2009 software (Zeiss) was used to construct composite images from each optical series by combining the images recorded through both channels.

For diaminobenzidine (DAB) immunoperoxidase staining, the sections were washed in PB after binding of the mouse anti-α actinin primary antibodies (1:500, Sigma) and then incubated with biotinylated horse anti-mouse secondary antibodies (1:200; Vector Laboratories) that were detected using the Vectastain ABC immunoperoxidase kit (Vector Laboratories). Antibody labeling for conventional light microscopy was visualized with 0.05% 3,3 diaminobenzidine tetrahydrochloride (Sigma,) and 0.01% hydrogen peroxide. For light microscopy, the sections were rinsed in PB, mounted on glass slides, dehydrated, cleared with xylene, and coverslipped.

Some sections immunostained for α-actinin were processed for electron microscopy, following the same protocol as described above except for the lower concentration of Triton-X in the buffers (0.05%). Once the immunohistochemical staining had been completed, the sections were postfixed in 2% glutaraldehyde in PB for 1 h, treated with 1% osmium tetroxide for 40 min, dehydrated, and flat embedded in Araldite resin. Plastic-embedded sections were studied by correlative light and electron microscopy, as described in detail elsewhere (DeFelipe and Fairén 1993). Briefly, sections were photographed under the light microscope and then serially cut into semithin (2-μm thick) sections on a Leica ultramicrotome. The semithin sections were stained with 1% toluidine blue in 1% borax, examined under the light microscope, and then photographed to locate the region of interest. Serial ultrathin sections (50- to 70-nm thick) were obtained from selected semithin sections on a Leica ultramicrotome, and they were collected on formvar-coated single-slot nickel grids and stained with uranyl acetate and lead citrate. Digital images were captured at different magnifications on a Jeol JEM-1011 transmission electron microscope (JEOL Inc., MA) equipped with a 11 Megapixel Gatan Orius CCD digital camera.

In all cases, Adobe Photoshop CS4 software was used to generate the figures (Adobe Systems Inc., San Jose, CA). Controls were included in all the immunocytochemical procedures, either by replacing the primary antibodies with preimmune goat or horse serum in some sections, by omitting the secondary antibodies, or by replacing the secondary antibody with an inappropriate secondary antibody. No significant immunolabeling was detected under these control conditions.

Neuronal Cultures

Hippocampal neurons were obtained from E17 mouse embryos and prepared as described previously (Banker and Goslin 1988). Briefly, after dissection of the hippocampus, the tissue was washed 3 times in Ca^{2+}/Mg^{2+}-free hanks' balanced salt solution (HBSS) and digested for 15 min in the same solution containing 0.25% trypsin. The tissue was again washed 3 times in Ca^{2+}/Mg^{2+}-free HBSS, and it was then dissociated with a fire-polished Pasteur pipette. The cells were recovered, counted, and resuspended in plating medium (Minimum essential medium + 10% Horse Serum and 0.6% glucose) and seeded at a density of 50 000/cm^2 on polylysine-coated coverslips (1 mg/mL). After 2 h, the medium was replaced with neuronal culture medium (Neurobasal medium + B-27 and glutamax I) and to maintain the neurons for 21 days in vitro (DIV); the cells were transferred to 60 mm plates containing astrocyte monolayers cultured in neuronal medium over the previous 24 h. 1-β-D-arabinofuranosylcytosine (AraC) was added (5 μM) after 2 days in culture to prevent astroglial cell growth. In some cases, neurons were treated between 15 and 17 DIV with 5 μM Cytochalasin D (Sigma). Before analyzing the neurons after different times in culture, the cultures were rinsed and fixed in 4% paraformaldehyde for 20 min.

After fixing the neurons, they were analyzed by immunocytochemistry. After washing in phosphate-buffered saline (PBS), the coverslips were treated with 50 mM NH_4Cl and incubated in blocking buffer for 45 min (PBS plus 0.22% gelatin and 0.1% Triton X-100). After blocking nonspecific binding, the coverslips were incubated for 1 h at room temperature with the primary antibodies diluted in blocking buffer. Chicken anti-MAP2 (1:5000, Abcam ab5352, Cambridge, UK) and rabbit anti-phospho-IκBα (1:250, Cell Signaling S2859, Beverly, MA) primary antibodies were used either alone or in combination with the primary antibodies indicated above. Secondary antibodies coupled to Alexa 488, Alexa 594, or Alexa 647 were used and raised in donkey or chicken against mouse, rabbit, or goat antibodies (Invitrogen, Carlsbad, CA). In some neurons, actin filaments were stained with Alexa 488 phalloindin (1:100, Invitrogen, A-12379) alone or in combination with α-actinin or synaptopodin immunostaining. 4′,6-diamidino-2-phenylindole (DAPI) (1 μg/mL, Calbiochem, 268298, Nottingham, UK) was used to counterstain the nuclei. After staining, the coverslips were mounted in Fluoromount G (Southern Biotech, Birmingham, AL), and images were obtained using a DP70 camera attached to an Olympus BX51 fluorescence microscope or a laser scanning confocal microscope (Zeiss 710).

Results

Presence of α-actinin and Synaptopodin in the AIS of Neocortical and Hippocampal Pyramidal Neurons

Light Microscopy

When immunostaining for the synaptopodin protein was examined in both the neocortex and hippocampus (Figs 1 and 2), the protein was seen to be distributed in small punctae that in previous studies were considered to correspond to dendritic spines (Deller et al. 2003, 2007; Vlachos et al. 2009).

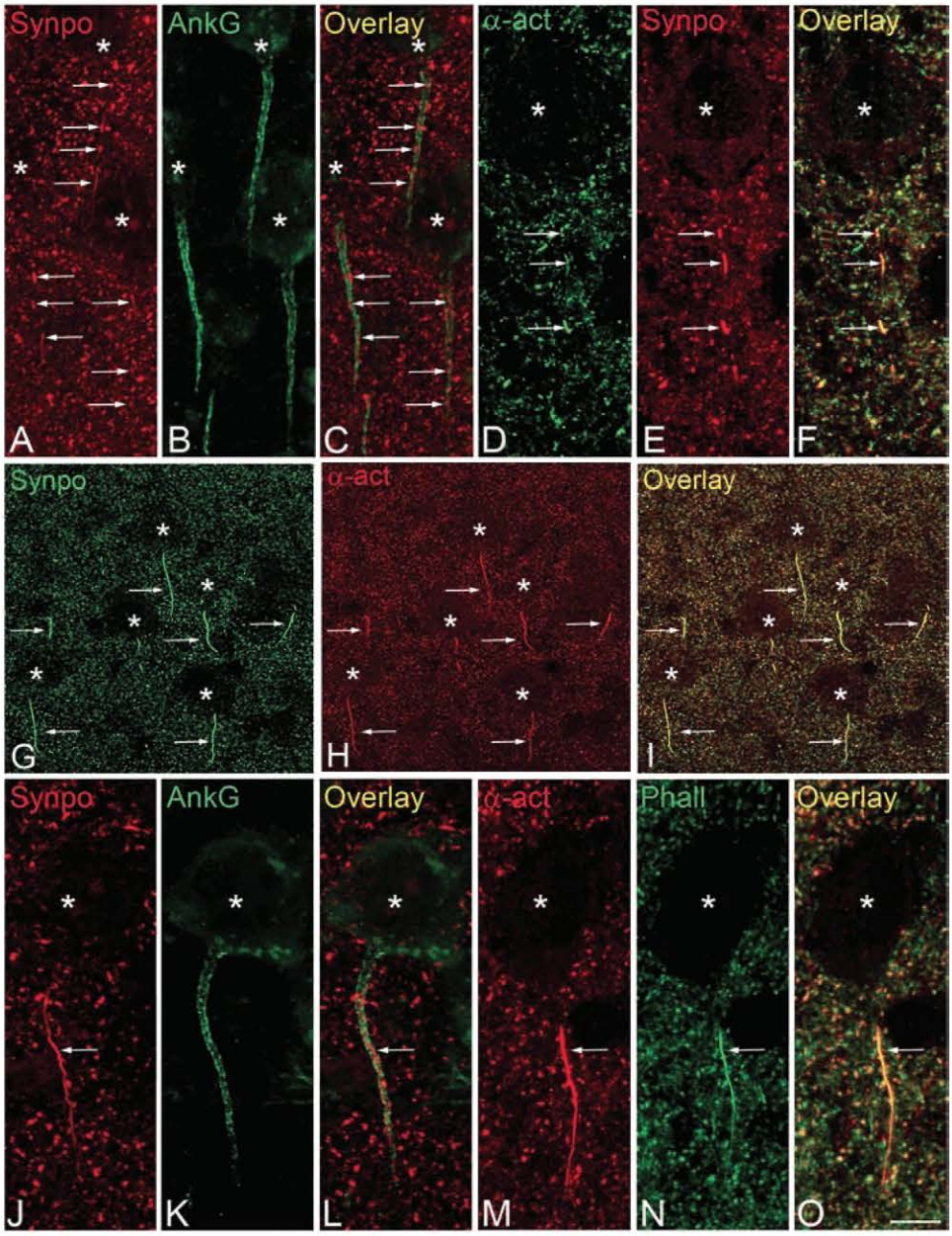

Figure 1. Photomicrographs from sections of the rat (*A–C, J–L*) or mouse (*D–I, M–O*) parietal neocortex showing the distribution of synaptopodin (synpo) and α-actinin-2 in the AIS. Note the presence of large clusters of synaptopodin immunostaining in the AIS, which was identified by immunostaining for ankyrin G. Note that the number and length of synaptopodin-ir elements varies between different neuronal populations of pyramidal cells (layer III in *A–F* and layer V in *G–O*). α-actinin-2 and synaptopodin colocalize to a large extent in the cisternal organelle of the AIS in neocortical pyramidal cells (*D–I*). *M–O* show the presence of α-actinin (*M*) and thick actin filaments, as revealed by phalloidin staining (*N*), in a long rod-shaped element in the AIS of layer V pyramidal cells. Scale bar = 6 μm in *A–F* and *J–O* and 16 μm in *G–I*.

In layer III of the neocortex and in the CA1 region, dual immunofluorescence staining for synaptopodin and ankyrin G revealed the presence of elongated elements that were immunoreactive (-ir) for synaptopodin and that were larger than those located in the dendritic spines. Since these structures also contained the AIS marker ankyrin G, synaptopodin was considered to be localized to the AIS (Fig. 1*A–C,J–L*). Synaptopodin-ir AIS elements were particularly prominent in a population of layer V pyramidal neurons where a single rod-shaped synaptopodin-ir process extended through almost the whole length of the AIS (Fig. 1*G,J–L*). These rod-shaped synaptopodin-ir processes were frequently a continuation of, and probably arose from, similar elongated structures in the cytoplasm at the base of the pyramidal soma that switched direction to enter the axon hillock and to funnel into the AIS (Fig. 2*A–C*). These rod-shaped synaptopodin-ir processes were more frequently found in the somatosensory and motor areas than in other areas of the frontal parietal, temporal, and occipital neocortex, where they were very scarce.

Immunostaining for α-actinin revealed a similar pattern of immunostaining to that of synaptopodin, both in the neocortex and hippocampal CA1 (Figs 1 and 2). In the AIS, α-actinin-ir elements largely colocalized with synaptopodin in double-labeling experiments, although they were seen variably in the different neuronal populations examined. Antibodies directed against α-actinin labeled the cisternal organelle in layer III

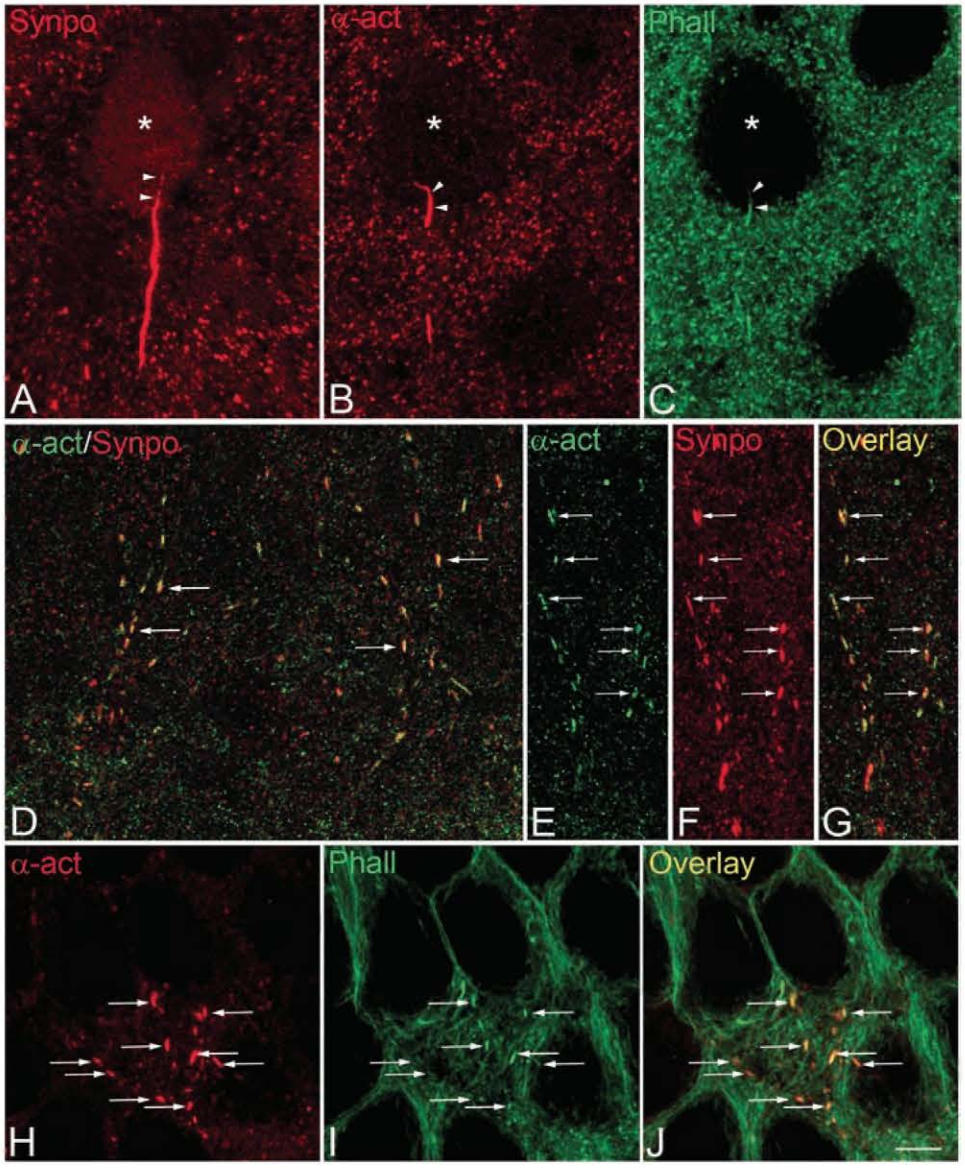

Figure 2. Photomicrographs from layer V of the mouse parietal neocortex (*A–C*) and CA1 hippocampal region (*D–J*) showing the distribution of synaptopodin (synpo), α-actinin-2, and actin in the AIS. *A–C* show that the rod-shaped element in layer V pyramidal cells, immunostained for synaptopodin (*A*), or double stained for α-actinin and actin/phalloidin (*B–C*), is a continuation of the labeled elements in the cytoplasm at the base of the pyramidal soma that pass through the axon hillock and enter the AIS (arrowheads). Note the large extent of α-actinin-2 and synaptopodin colocalization in the cisternal organelle of the AIS (*D–G*, arrows). *H–J* show the presence of α-actinin (*H*) and actin filaments (as revealed by phalloidin staining: *I*) in the AIS of CA1 pyramidal cells (arrows). Scale bar = 7.5 μm in *A*, 10.5 μm in *B*, 5.7 μm in *D*, and 4.7 μm in *E–J*.

neocortical (Fig. 1*D–F*) and CA1 (Fig. 2*D–G*) pyramidal cells and the rod-shaped element in layer V pyramidal neurons (Figs 1*G–L* and 2*A–C*).

Double staining with antibodies directed against α-actinin and Alexa Fluor 488–labeled phalloidin demonstrated that actin filaments associated with α-actinin-ir structures in the AIS. This association included the rod-shaped elements in the AIS of layer V pyramidal cells (Figs 1*M–O* and 2*B,C*) and the elements of the cisternal organelle in CA1 pyramidal cells (Fig. 2*H–J*).

Electron Microscopy

Pre-embedding immunoperoxidase labeling and correlative light and transmission electron microscopy (TEM) were used in ultrastructural studies to analyze the subcellular distribution of α-actinin in the AIS (Figs 3 and 4). Although the α-actinin immunoperoxidase reaction product was evident in dendritic spines and AIS, we focused our attention here on the AIS. Indeed, α-actinin was seen to associate with rod-shaped structures in the AIS of layer V neocortical neurons (Fig. 3) and in puncta in the stratum pyramidale of CA1 hippocampal neurons (Fig. 4). This pattern was first identified in vibratome sections (50-μm thick, Fig. 3*A*), which were then embedded in araldite to obtain semithin sections (2-μm thick, Figs 3*B* and 4*A*) that were studied by light microscopy. After selecting the field of interest that included the α-actinin-ir AISs, the semithin sections were embedded in araldite to generate ultrathin sections that could be studied by TEM (Figs 3*C–E* and 4*B–I*). At the ultrastructural level, the AISs were identified on the basis of the presence of the undercoating beneath the plasma membrane (arrowheads in Figs 3 and 4) and through the microtubule bundles.

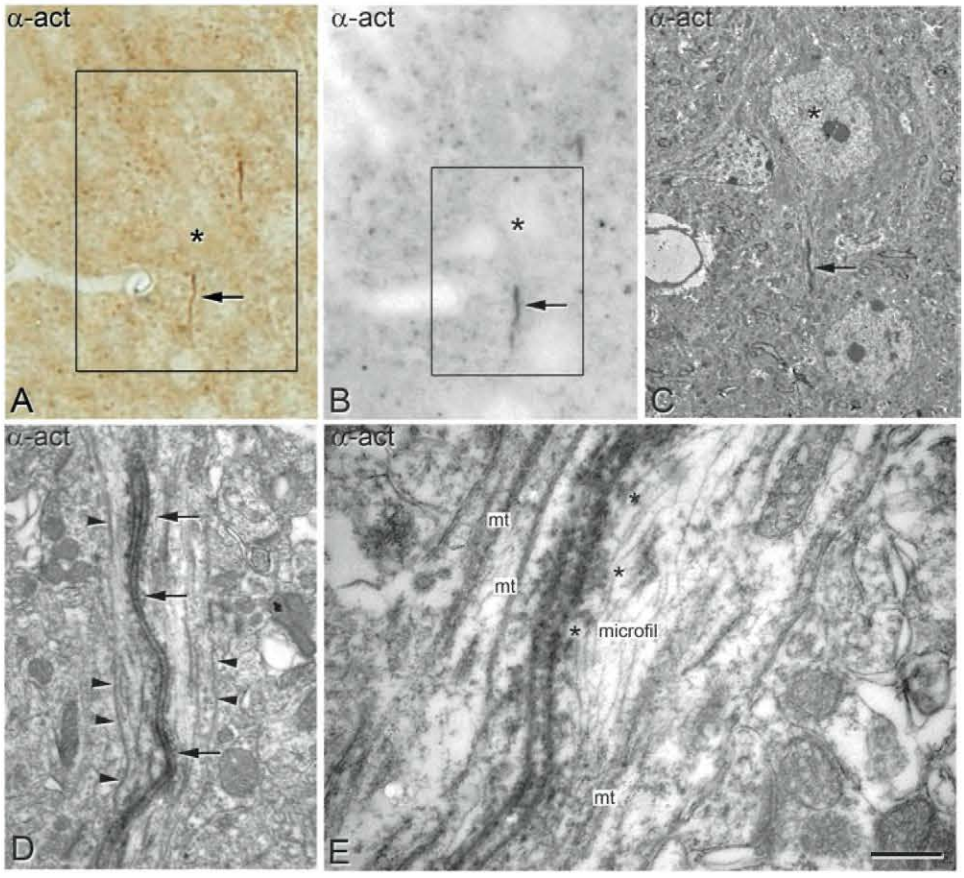

Figure 3. Correlative light and electron microscopy images showing the distribution of α-actinin in the cisternal organelle of layer V pyramidal cells from the mouse parietal neocortex. The α-actinin-ir rod-shaped structure in the AIS of layer V pyramidal neurons (AIS) was identified by light microscopy in vibratome sections (50 μm, *A*) and in semithin sections (2 μm) and by electron microscopy in ultrathin sections (70 nm, *C–E*). The boxed regions in *A* and *B* are shown at higher magnification in *B* and *C*, respectively. Note that the α-actinin reaction product is found in a central tubular structure that extends along the length of the AIS (arrows in *D*), and the patches of α-actinin reaction product (asterisks) are associated with microfilaments. Arrowheads point to the AIS undercoat. mt: microtubules. Scale bar: 16 μm in *A*, 11 μm in *B*, 6 μm in *C*, 800 nm in *D*, and 270 nm in *E*.

In the AIS of layer V neocortical pyramidal neurons (Fig. 3), the distribution of α-actinin varied with respect to that in CA1 cells (Fig. 4), and the α-actinin-ir rod-like structures do not correspond to the cisternal organelle. Rather, α-actinin appeared to be associated with a very prominent elongated structure that extended throughout the length of the AIS, parallel to the axon's longitudinal axis (Fig. 3*D,E*). We refer to this structure as the "giant saccular organelle," which was made up of a discrete number of long tubules and flattened sacs orientated parallel to the long axis of the axon and located between the microtubules and microfilaments. The α-actinin DAB reaction product was observed between the sacs and often, as discontinuous patches along the surfaces of this giant saccular organelle. In addition, bundles of filaments with no α-actinin but preferentially orientated parallel to the giant saccular organelle were frequently found to associate laterally or to terminate in patches of α-actinin (Fig. 3*E*). The opposite end of these filaments was often observed to associate with either AIS microtubules or the cytoplasmic side of the plasmalemma. In cross section, these filaments were less than 10 nm in diameter, and the pattern of phalloidin staining in the AIS described above suggests that they were actin microfilaments that might participate in the stabilization of the giant saccular organelle within this population of layer V pyramidal neurons.

In the AIS of CA1 pyramidal neurons and in accordance with previous studies, the cisternal organelle was made up of stacks of flat membranous cisterns with a narrow lumen alternating with electron dense material. The outermost cisternae associated with the inner aspect of the plasma membrane. The α-actinin DAB reaction product was found at different points along the AIS (Fig. 4*G*), and it was associated with the dense plates of material located between the membranous cisterns of the cisternal organelle (Fig. 4). By contrast, it was generally absent from other smooth endoplasmic structures in the AIS.

Cultured Hippocampal Neurons

α-actinin Expression in the AIS

In hippocampal neurons cultured for 21 days, α-actinin was detected in the AIS, which was identified by pIκBα immunostaining. As in CA1 tissue, α-actinin labeling in the AIS clustered in numerous small patches along the length of the AIS (Fig. 5*A–H*), which probably corresponded to the cisternal organelle. Large and round or slightly elongated α-actinin-ir elements were enriched in the AIS but not in the more distal regions of the axon or in dendritic processes. Due to the similar distribution of α-actinin and synaptopodin in the AIS (Bas Orth et al. 2007; Sánchez-Ponce et al. 2011b), we performed double staining to assess whether they might colocalize. Indeed, α-actinin largely colocalized with synaptopodin in the vast majority of neurons, suggesting a structural and/or functional association (Fig. 5*E–H*).

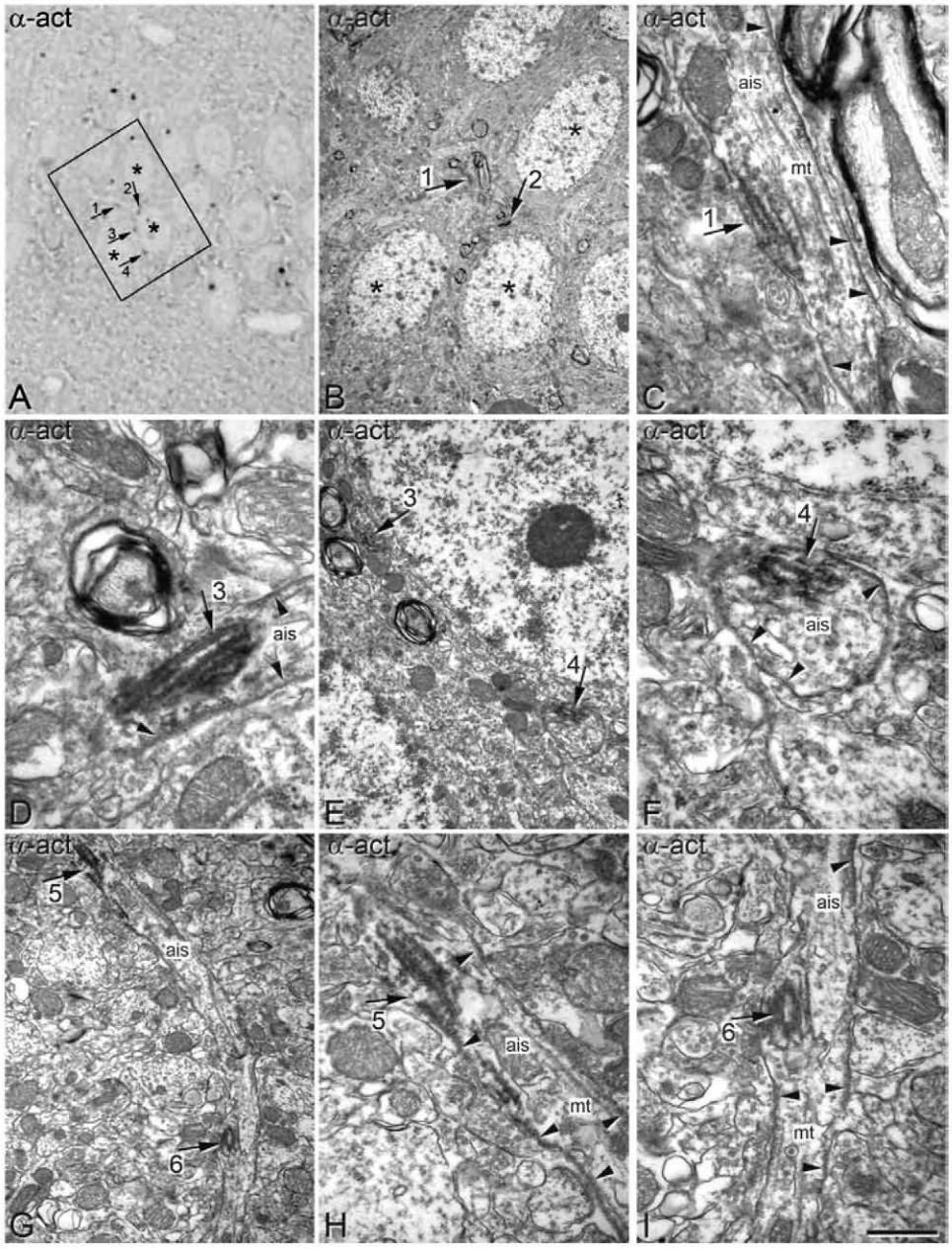

Figure 4. Correlative light and electron microscopy showing the distribution of α-actinin in the cisternal organelle of the AIS in CA1 hippocampal pyramidal cells. Numerous large puncta of α-actinin immunostaining were identified by light microscopy (boxed regions in *A*) and are shown at higher magnification in different ultrathin sections (*B* and *E*). *C–D* and *F* are higher magnifications of *B* and *E*, respectively. *G* shows 2 α-actinin-ir puncta (5 and 6) corresponding to the cisternal organelles of a single AIS shown at higher magnification in *H* and *I*. Note that the α-actinin reaction product associates with the dense plates between the membranous cisterns of the cisternal organelles. Asterisks label the position of neuronal cell bodies. ais, axon initial segment; mt, microtubules. Scale bar: 17 μm in *A*; 6 μm in *B*; 620 nm in *C*; 500 nm in *D*, *F*, *H*, and *I*; 1.6 μm in *E*; and 1.3 μm in *G*.

Developmental Expression of α-actinin in the AIS

We studied the expression and localization of α-actinin in cultured hippocampal neurons at different stages of development (1, 3, 5, 8, 10, 13, 15, 18, and 21 DIV: Fig. 6). In this model, an axon first appears in these cells after 24–36 h in culture (Banker and Goslin 1988), and before axon outgrowth, mild α-actinin immunostaining was observed in the soma with more intense staining at the tips of neurites, as reported previously for synaptopodin (Sánchez-Ponce et al. 2011b). During the first week in vitro, α-actinin was virtually absent from the AIS of neurons (Fig. 6*A–C*), after which the proportion of neurons with large particles along the length of the AIS, containing α-actinin, increased progressively as development proceeded (0% at 24 and 72 h, 2.21 ± 0.84% at 5 DIV, 9.97 ± 3.12% at 8 DIV, 24.21 ± 2.73% at 10 DIV, 31.01 ± 2.3% at 13 DIV, 40.31 ± 0.71% at 15 DIV, 42.87 ± 1.62% at 18 DIV, and 47.76 ± 2.90% at 21 DIV; data obtained from 3 separate experiments where $n \geq 100$ for each time point and experiment: Fig. 6). In addition, from around 15 DIV, synaptopodin-ir puncta were observed in dendritic processes, probably corresponding to dendritic spines where α-actinin has been located previously (Nakagawa et al. 2004).

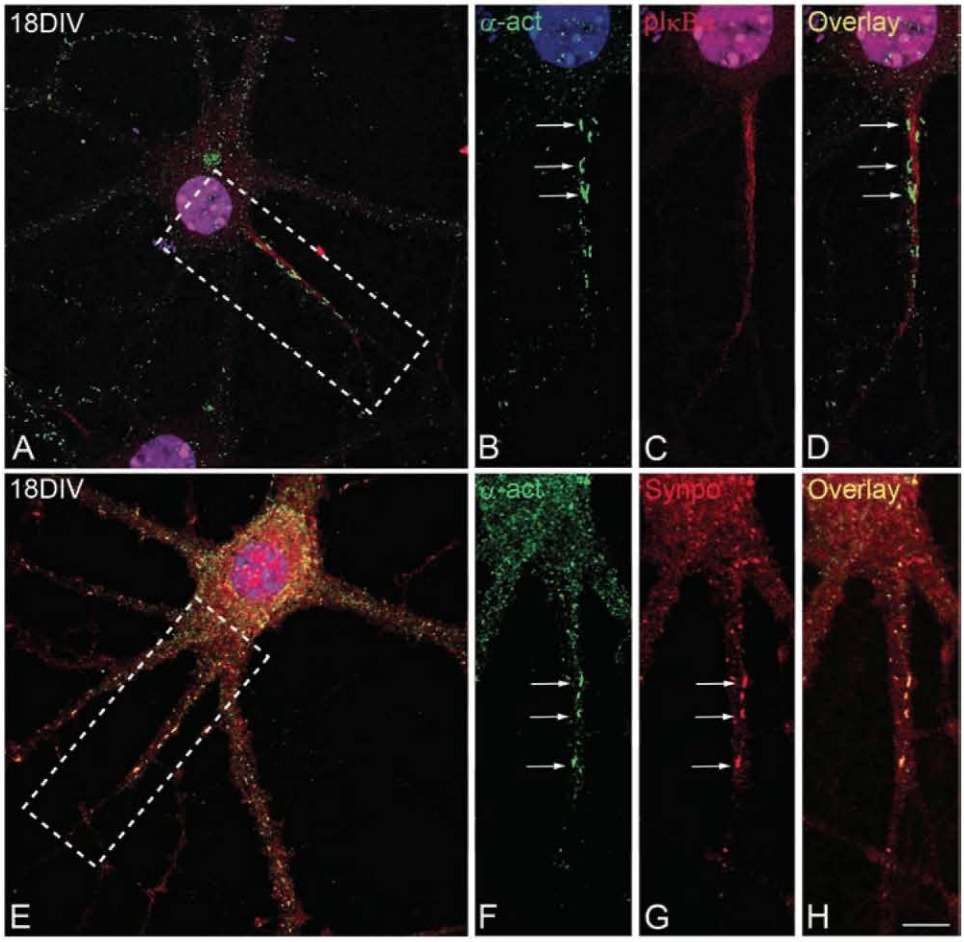

Figure 5. Confocal microscopy photomicrographs showing hippocampal neurons cultured for 18 days and dual immunostained for α-actinin-2 (green) and pIκBα (red) in *A–D*, and for α-actinin-2 (green) and synaptopodin (red) in *E–H*. Higher magnifications of the boxed regions of *A* and *E* are shown in *B–D* and *F–H*, respectively. Note the presence of large clusters of α-actinin-2 immunostaining in the initial segment of a single process emerging from the soma, identified as the AIS by pIκBα immunostaining. Note the large extent of α-actinin-2 and synaptopodin colocalization in the cisternal organelle microdomains of the AIS (*E–H*). Scale bar = 9.5 μm in *A* and *E* and 3.5 μm in *B–D* and *F–H*.

The Clustering of α-actinin in the AIS Depends on the Actin Cytoskeleton

The cisternal organelle was recently shown to be stabilized by the actin cytoskeleton since depolymerization induced by cytochalasin D affects both the structural and neurochemical features of the cisternal organelle (Sánchez-Ponce et al. 2011b). We analyzed the distribution of α-actinin in the AIS after treatment with the actin-depolymerizing agent cytochalasin D (Figs 7–9) to determine whether actin filaments might stabilize the cisternal organelle and the concentration of α-actinin in the AIS. Under our conditions, Cytochalasin D treatment effectively disrupted the actin cytoskeleton, as witnessed by the change in the patterns of phalloidin staining when compared with control neurons (Fig. 7*A,B*), although the general morphology of neurons does not seem to be affected, as revealed by MAP immunostaining (Fig. 7*C,D*). Indeed, Cytochalasin D altered phalloidin staining in both the somatodendritic domain and in axons, which were considered as individual MAP2-negative processes exiting the cell body (Fig. 7*E–J*). The shape of the α-actinin-ir elements was also affected, changing from round to elongated structures, and increasing in length in neurons treated with cytochalasin D (Fig. 8). These changes not only affected the α-actinin-ir elements in the AIS, as identified by pIκBα immunostaining, but also those located in the cell body and dendritic processes (Fig. 8*G,H*). In addition, α-actinin colocalized fully with synaptopodin in AIS processes of control neurons (Fig. 8*D–F*) and in the elongated structures formed in the different neuronal compartments in the presence of cytochalasin D, including the AIS (Fig. 8*H,L–N*).

These results indicate that the integrity of the actin cytoskeleton does not seem to be required for the structural and/or functional association of α-actinin and synaptopodin. However, they show that in addition to synaptopodin, the strategic position of α-actinin is affected by the polymerized state of the actin microfilaments and that the actin cytoskeleton plays an active role in maintaining the morphological features of the cisternal organelle in the AIS. In keeping with the results from brain sections, phalloidin-labeled actin filaments were associated with the α-actinin-ir in the AIS of control hippocampal cultured cells (Fig. 9*A–D,I–L*). Moreover, cytochalasin D altered the patterns of phalloidin staining in different cell regions, including the AIS, reflecting the effect of F-actin depolymerization in our conditions (Fig. 9*E,H,M,Q*). These modifications were associated with the elongation of the synaptopodin-ir (Fig. 9*E–H*) and α-actinin-ir AIS (Fig. 9*M–Q*), further supporting the involvement of the actin cytoskeleton in the maintenance of the morphological features of the cisternal organelle in the AIS.

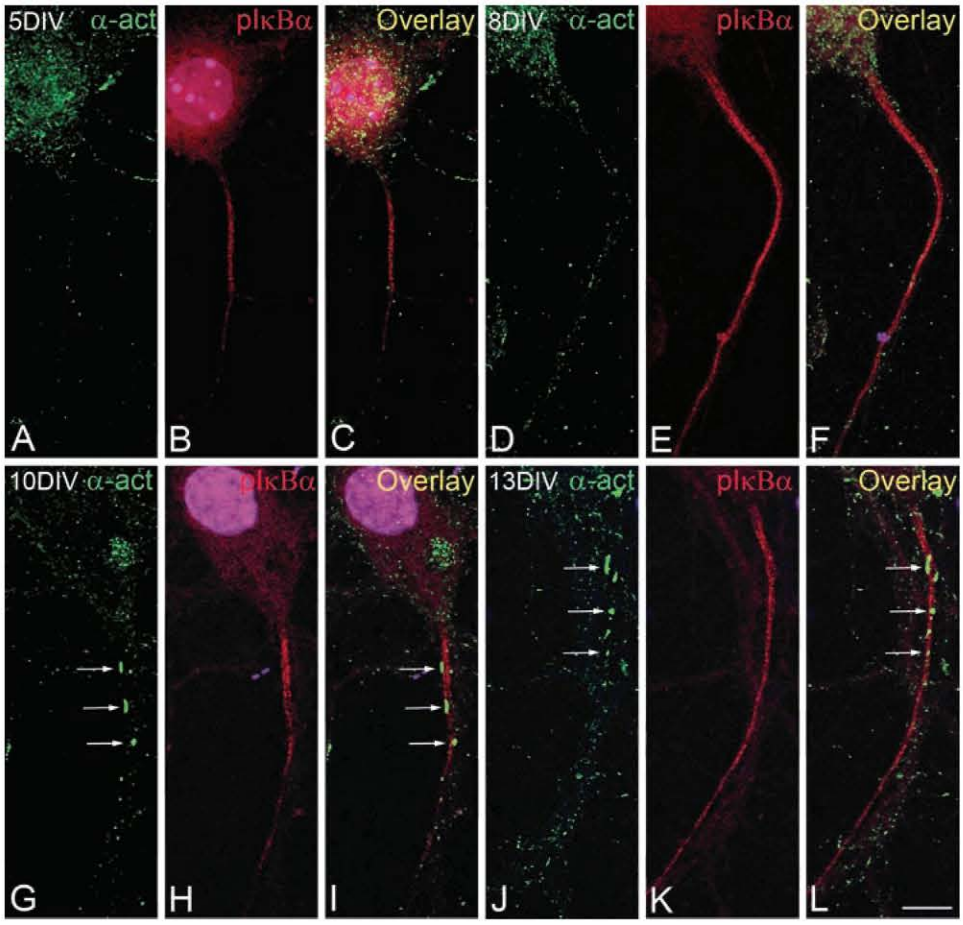

Figure 6. Maturation of α-actinin-2 expression in developing hippocampal neurons. Hippocampal neurons were grown in vitro at low density for different lengths of time (5000/cm^2), fixed in 4% paraformaldehyde, and doubled stained with antibodies against α-actinin-2 (green) and pIκBα (red), before they were counterstained with DAPI (blue). Images show diffuse α-actinin-2 immunostaining in the cell bodies. From 10 DIV onward (*G–L*), α-actinin-2 clustered in large and intensely stained patches in the initial segment of a single-process emerging from the soma, which was identified as the AIS (arrows) by the presence of pIκBα. Also note that α-actinin-2 is absent from the AIS during the first 10 DIV. Scale bar indicates 7 μm.

Discussion

The α-actinins accumulate in different types of cell junctions, most notably at focal adhesions. These proteins are associated to the submembranous cytoskeleton where in conjunction with actin, α-actinin creates isotropic networks of short-branched bundles of actin filaments (Wachsstock et al. 1993; Clark and Brugge 1995; Pelletier et al. 2003; Otey and Carpen 2004). In addition, this protein can interact with a variety of cytoskeletal- and membrane-associated proteins (Blanchard et al. 1989). Among other α-actinin isoforms, α-actinin-2 (the sarcomeric form) is expressed in the brain (Wyszynski et al. 1997; Walikonis et al. 2000, 2001) as well as being widely expressed in skeletal and cardiac muscle fibers (Lek et al. 2010). In the neocortex and hippocampus, prominent α-actinin-2 expression has been described in a laminar and regional manner, mainly in punctuate structures in the neuropil and in the cell body of specific interneuron populations (Wyszynski et al. 1998; Ratzliff and Soltesz 2001; Price et al. 2005; Kubota et al. 2011). Punctuate structures immunoreactive for α-actinin-2 mainly correspond to the dendritic spines of cortical principal cells in which α-actinin-2 accumulates in the postsynaptic density and the spine apparatus (Wyszynski et al. 1998).

In addition to dendritic spines, elongated puncta of α-actinin-2 were evident as dashed lines extending a short distance from the base of pyramidal cells (Wyszynski et al. 1998), which were proposed to correspond to either the AIS or intradendritic structures (Wyszynski et al. 1998). The colocalization with AIS markers here demonstrates that α-actinin-2 is a component of the AIS in different populations of principal neurons in the rodent neocortex and hippocampus. Given its ability to cross-link actin filaments, α-actinin-2 could be an important structural component of the cytoskeleton potentially stabilizing the cisternal organelle in the AIS. Here, we show that α-actinin largely colocalizes with synaptopodin and actin filaments, indicative of a functional association between them. At the ultrastructural level, α-actinin-2 distributes in the typical cistenal organelle of the AIS of CA1 pyramidal neurons, where it is associated with the dense plates of material located between the membranous cisterns. A similar distribution was previously described for synaptopodin (Bas Orth et al. 2007), suggesting that both proteins may contribute to the structural maintenance of the cisternal organelle.

Another interesting finding of this study is that the giant saccular organelle is only found in the AIS of a subpopulation of layer V pyramidal neurons, a prominent specialization in these particular neurons. Although contacts between the giant saccular organelle and the AIS plasma membrane were occasionally found, it seems to correspond to a specialization

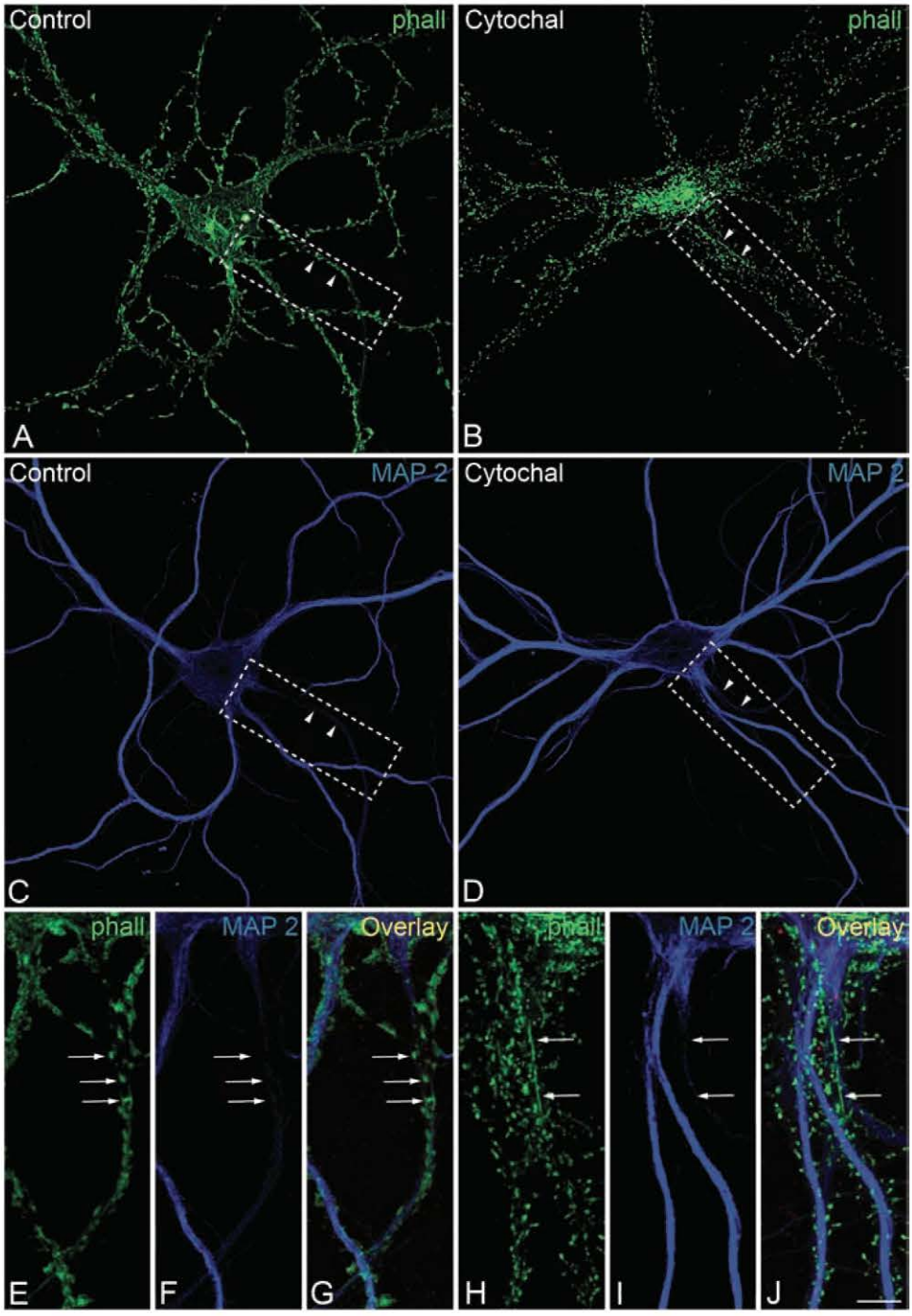

Figure 7. Confocal images showing a control cultured hippocampal neuron (*A*, *C*, and *E–G*) and a neuron treated with the actin-depolymerizing agent, cytochalasin D (*B*, *D*, and *H–J*). Actin filaments were stained with alexa 488-phalloidin in the cells (*A*, *B*, *E*, and *H*), or they were immunostained with antibodies to MAP 2 (*C*, *D*, *F*, and *I*) to reveal their morphology. Boxed regions in *A–D*, including the MAP2 negative AIS (arrowheads), are shown at higher magnification in *E–J*. Despite the apparent lack of gross morphological alterations, note the modified pattern of phalloidin staining in cytochalasin D treated neurons when compared with control neurons, both in the somadendritic domain and the AIS (arrows in *E–J*).

of the central component of the axonal smooth endoplasmic reticulum (Peters et al. 1991), comprised of long tubules and sacs of irregular shape oriented parallel to the long axis of the axon. This structure is mainly located in a central position within the AIS, and it extends throughout its length. These features contrast with those of the cisternal organelle, present in the principal neurons of a variety of neocortical areas and layers, and in regions of the hippocampus, which may represent the peripheral component of the axonal smooth endoplasmic reticulum (Peters et al. 1991). Indeed, this organelle is made up of stacks of membranous cisternae, the outermost of which are attached to the axonal plasma membrane, often associated with regions of the AIS that receive synaptic contacts (i.e., Kosaka 1980). In contrast to the cisternal organelle, the giant saccular organelle also appears to extend through the axon hillock and the cytoplasm at the base of the pyramidal soma, and it could be continuous with endoplasmic reticulum of the cell body. These observations

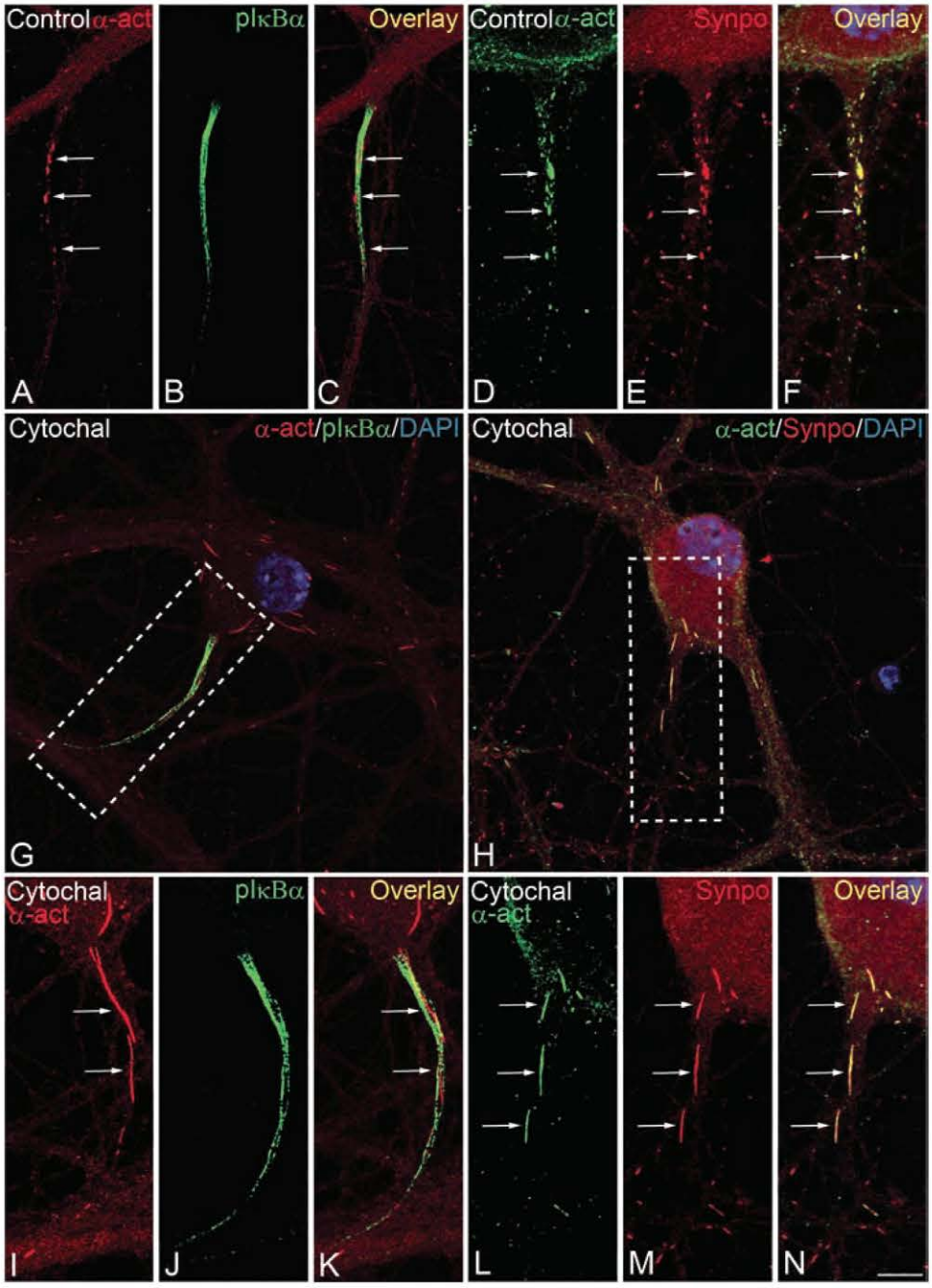

Figure 8. Dependence on the actin cytoskeleton. Confocal images showing that the morphological features of the synaptopodin (synpo) (*H*, *L–N*) and α-actinin-2 (*G–N*) positive elements in the AIS are affected by Cytochalasin D treatment of hippocampal neurons when compared with control cells (*A–F*). Note the decrease in the number of synaptopodin-ir elements in the AIS and the increase in their length (*D*). Higher magnifications of the boxed regions of *G* and *H* are shown in *I–K* and *L–N*, respectively. Scale bars = 6 μm in *A–F* and *I–N* and 9 μm in *G* and *H*.

further emphasize the important differences in AIS organization between neuronal populations (e.g., see Lorincz and Nusser 2008). The function of the giant saccular organelle in the AIS of layer V neurons remains unknown and whether it is involved in storing and regulating Ca^{2+} release, as proposed for the cisternal organelle in other neuronal populations (Benedeczky et al. 1994, Bas Orth et al. 2007; Sánchez-Ponce et al. 2011b), is an interesting possibility that should be evaluated in further studies.

The giant saccular organelle expresses synaptopodin and α-actinin and, at the ultrastructural level, numerous microfilaments associate with patches of α-actinin-2. These microfilaments were often seen to contact adjacent microtubules and the cytoplasmic face of the plasma membrane, and they would appear to participate in the structural support provided to the giant saccular organelle. This organization is reminiscent of the situation in muscle cells in which α-actinin forms a complex with other proteins, including myopodin (the equivalent to synaptopodin in muscle cells) in the Z disks. In these cells, α-actinin participates in Z-disk assembly, the antiparallel cross-linking of actin filaments from adjacent sarcomeres, and in associating and stabilization the nascent myofibrils to the

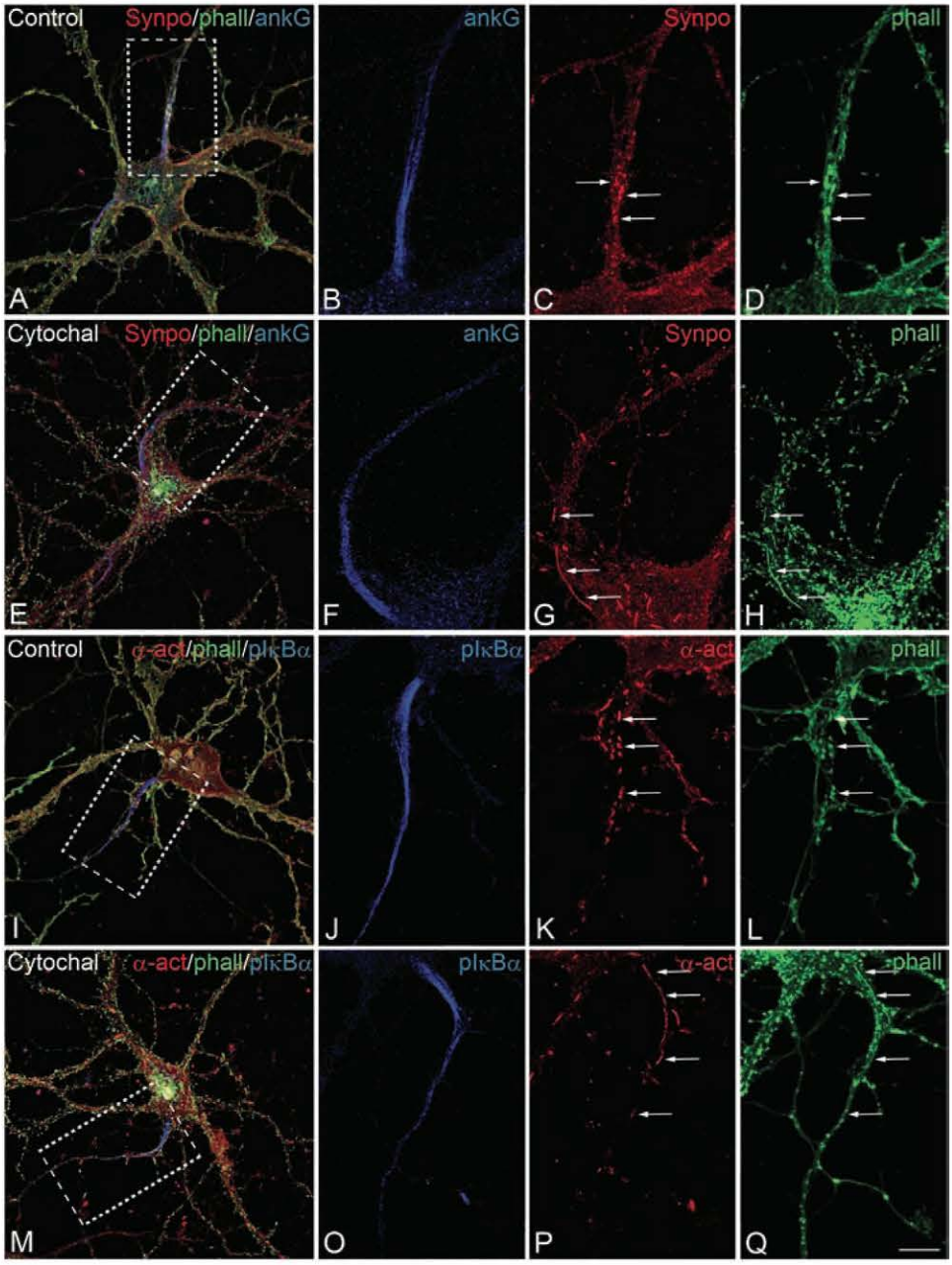

Figure 9. Confocal images showing the relationship between AIS actin filaments, labeled with Alexa 488–coupled phalloidin and the cisternal organelle immunoreactive for synaptopodin (synpo) or α-actinin-2. Note that alterations to the actin cytoskeleton induced by cytochalasin D, as revealed by changes in the distribution of phalloidin-labeled F-actin, are paralleled by the elongation of the synaptopodin-ir or α-actinin-2-ir cisternal organelle in the AIS. Scale bar represents 17 μm in *A*, *E*, *I*, and *M* and 6.5 μm in *B–D*, *F–H*, *J–L*, and *O–Q*.

sarcolema (Weins et al. 2001; Faul et al. 2007; Schroeder et al. 2008; Linnemann et al. 2010).

In Vitro Development and Stabilization of the Cisternal Organelle

In the light of earlier observations (Sánchez-Ponce, et al. 2011a,b), we demonstrate here that α-actinin and synaptopodin colocalize to a large extent and that they appear concomitantly during the development in the AIS of cultured mouse hippocampal neurons. These proteins are only present at the AIS well after it is organized and expresses other molecules relevant for its development and activity, such as pIκBα, CK2, ankyrin G, and Na^+ channels (Sánchez-Ponce et al. 2008; 2011a,b). This is consistent with previous studies in cultured hippocampal neurons in which a punctuate distribution of α-actinin-2 commences at 10 DIV (Rao et al. 1998). Indeed, data from the rat hippocampus and neocortex indicate that although α-actinin-2 is expressed as early as P1, its expression and distribution augments progressively and matures during the first 2 postnatal weeks (Wyszynski et al. 1998; Ratzliff and Soltesz 2001). The delayed expression of α-actinin-2 and synaptopodin in the AIS seen here may be related to the late appearance of the cisternal organelle in cultured hippocampal neurons, which coincides with the appearance of IP_3R1 and annexin 6 in the AIS

(Sánchez-Ponce et al. 2011b) and that could be related to the maturation of the ability to regulate Ca^{2+} in the AIS.

The scaffolding protein ankyrin G is an essential organizer of AIS assembly (Zhou et al. 1998; Jenkins and Bennett 2001; Hedstrom et al. 2008; Sobotzik et al. 2009; Rasband 2010; Sánchez-Ponce et al. 2011b), and the development of the cisternal organelle is also an ankyrin G–dependent process. Indeed, the expression of synaptopodin, IP_3R1, and annexin 6 is impaired in the AIS of ankyrin G–deficient cultured hippocampal neurons (Sánchez-Ponce et al. 2011b). In addition to ankyrin G, the formation of the cisternal organelle is also critically dependent upon the presence of synaptopodin between the membranous cisterns (Bas Orth et al. 2007). Moreover, the accumulation of annexin 6 and IP_3R1 in AIS microdomains is also dependent on the integrity of the actin cytoskeleton (Sánchez-Ponce et al. 2011b). Indeed, the actin-depolarizing agent cytochalasin D reduces the number of synaptopodin positive processes in the AIS and alters their shape (Sánchez-Ponce et al. 2011b). Likewise, the morphological features of the α-actinin-2-ir elements in the AIS of cultured hippocampal cells are also affected by cytochalasin D, in accordance with previous studies showing that F-actin is responsible for the anchoring and synaptic localization α-actinin-2 in dendritic spines (Allison et al. 2000). Together, this indicates that the actin cytoskeleton is implicated in the positioning, stabilization, and neurochemistry of the cisternal organelle. The relevance that this might have for the spatiotemporal regulation of Ca^{2+} concentrations in the AIS of principal hippocampal cells should be evaluated in further studies. As annexin 6 interacts with α-actinin (Mishra et al. 2011), F-actin interacts with IP_3Rs (Fujimoto et al. 1995), and actin polymerization modulates Ca^{2+} release from IP_3 sensitive stores (Wang et al. 2002), it is possible that synaptopodin and/or α-actinin in the AIS are involved in the interactions necessary to recruit IP_3R1 or annexin 6 to AIS microdomains.

The interaction of α-actinin and actin is dynamic (Hotulainen and Lappalainen 2006) and subject to regulation by PIP_2 (Fukami et al. 1992) and Ca^{2+} (Duhaiman and Bamburg 1984), the latter inhibiting the actin-binding activity of purified brain α-actinin (Duhaiman and Bamburg 1984). However, it remains to be clarified whether the activity-driven and Ca^{2+}-mediated AIS plasticity leading to structural changes in the length and position of the AIS (Kuba et al. 2010, Grubb and Burrone 2010a, 2010b) depends on the plastic changes in the cisternal organelle in which α-actinin-2 is involved.

Although the precise functions that α-actinin-2 fulfills in the AIS are unknown, it could participate in the anchoring of ion channels and receptors. Indeed, in cardiomyocytes, the correct membrane localization of small conductance Ca^{2+}-activated K^+ channels (SK2 or $K_{Ca}2.2$) is dependent on its interaction with α-actinin 2 (Lu et al. 2009). In neurons, α-actinin-2 links NMDA receptor subunits to the cytoskeleton, possibly modulating NMDA receptor function and localization in dendritic spines (Wyszynski et al. 1997; Allison et al. 1998; Zhang et al 1998; Krupp et al. 1999; Dunah et al. 2000; Rycroft and Gibb 2004). α-actinin-2 also binds to CaMKII (Walikonis et al. 2001), and in dendritic spines, the clustering of α-actinin-2 and CaMKIIα depends on F-actin (Allison et al. 1998, 2000). In the AIS, cross-linking by α-actinin-2 could also indirectly modulate the activity of any protein associated to the actin cytoskeleton, such as βIV spectrin, ankyrin G, VGSC (Rasband 2010), and the CaMKIIα kinase (Hund et al. 2010).

Funding

Ministerio de Ciencia e Innovación (SAF 2010-18218 to A.M., SAF 2009-12249-C02-02 to J.J.G., and SAF 2009-09394 to J.D.), Cajal Blue Brain Project, and Centro de Investigación Biomédica en Red de Enfermedades Neurodegenerativas (CIBERNED). D.S. is supported by an Formación de Profesorado Universitario fellowship from the Ministerio de Educación (Spain).

Notes

Conflict of Interest : None declared.

Allison DW, Chervin AS, Gelfand VI, Craig AM. 2000. Postsynaptic scaffolds of excitatory and inhibitory synapses in hippocampal neurons: maintenance of core components independent of actin filaments and microtubules. J Neurosci. 20:4545–4554.

Allison DW, Gelfand VI, Spector I, Craig AM. 1998. Role of actin in anchoring postsynaptic receptors in cultured hippocampal neurons: differential attachment of NMDA versus AMPA receptors. J Neurosci. 18:2423–2436.

Asanuma K, Kim K, Oh J, Giardino L, Chabanis S, Faul C, Reiser J, Mundel P. 2005. Synaptopodin regulates the actin-bundling activity of alpha-actinin in an isoform-specific manner. J Clin Invest. 115:1188–1198.

Banker G, Goslin K. 1988. Developments in neuronal cell culture. Nature. 336:185–186.

Bas Orth C, Schultz C, Muller CM, Frotscher M, Deller T. 2007. Loss of the cisternal organelle in the axon initial segment of cortical neurons in synaptopodin-deficient mice. J Comp Neurol. 504:441–449.

Bender KJ, Trussell LO. 2009. Axon initial segment Ca^{2+} channels influence action potential generation and timing. Neuron. 61:259–271.

Benedeczky I, Molnar E, Somogyi P. 1994. The cisternal organelle as a $Ca^{(2+)}$-storing compartment associated with GABAergic synapses in the axon initial segment of hippocampal pyramidal neurones. Exp Brain Res. 101:216–230.

Blanchard A, Ohanian V, Critchley D. 1989. The structure and function of alpha-actinin. J Muscle Res Cell Motil. 10:280–289.

Capani F, Martone ME, Deerinck TJ, Ellisman MH. 2001. Selective localization of high concentrations of F-actin in subpopulations of dendritic spines in rat central nervous system: a three-dimensional electron microscopic study. J Comp Neurol. 435:156–170.

Clark EA, Brugge JS. 1995. Integrins and signal transduction pathways: the road taken. Science. 268:233–239.

DeFelipe J, Fairén A. 1993. A simple and reliable method for correlative light and electron microscopic studies. J Histochem Cytochem. 41:769–772.

Deller T, Korte M, Chabanis S, Drakew A, Schwegler H, Stefani GG, Zuniga A, Schwarz K, Bonhoeffer T, Zeller R, et al. 2003. Synaptopodin-deficient mice lack a spine apparatus and show deficits in synaptic plasticity. Proc Natl Acad Sci U S A. 100:10494–10499.

Deller T, Orth CB, Del Turco D, Vlachos A, Burbach GJ, Drakew A, Chabanis S, Korte M, Schwegler H, Haas CA, et al. 2007. A role for synaptopodin and the spine apparatus in hippocampal synaptic plasticity. Ann Anat. 189:5–16.

Di Biase V, Obermair GJ, Szabo Z, Altier C, Sanguesa J, Bourinet E, Flucher BE. 2008. Stable membrane expression of postsynaptic CaV1.2 calcium channel clusters is independent of interactions with AKAP79/150 and PDZ proteins. J Neurosci. 28:13845–13855.

Duhaiman AS, Bamburg JR. 1984. Isolation of brain alpha-actinin. Its characterization and a comparison of its properties with those of muscle alpha-actinins. Biochemistry. 23:1600–1608.

Dunah AW, Wyszynski M, Martin DM, Sheng M, Standaert DG. 2000. alpha-actinin-2 in rat striatum: localization and interaction with NMDA glutamate receptor subunits. Brain Res Mol Brain Res. 79:77–87.

Faul C, Dhume A, Schecter AD, Mundel P. 2007. Protein kinase A, Ca^{2+}/calmodulin-dependent kinase II, and calcineurin regulate the

intracellular trafficking of myopodin between the Z-disc and the nucleus of cardiac myocytes. Mol Cell Biol. 27:8215–8227.
Fujimoto T, Miyawaki A, Mikoshiba K. 1995. Inositol 1,4,5-trisphosphate receptor-like protein in plasmalemmal caveolae is linked to actin filaments. J Cell Sci. 108:7–15.
Fukami K, Furuhashi K, Inagaki M, Endo T, Hatano S, Takenawa T. 1992. Requirement of phosphatidylinositol 4,5-bisphosphate for alpha-actinin function. Nature. 359:150–152.
Garrido JJ, Giraud P, Carlier E, Fernandes F, Moussif A, Fache MP, Debanne D, Dargent B. 2003. A targeting motif involved in sodium channel clustering at the axonal initial segment. Science. 300:2091–2094.
Grubb MS, Burrone J. 2010a. Activity-dependent relocation of the axon initial segment fine-tunes neuronal excitability. Nature. 465:1070–1074.
Grubb MS, Burrone J. 2010b. Building and maintaining the axon initial segment. Curr Opin Neurobiol. 20:481–488.
Hedstrom KL, Ogawa Y, Rasband MN. 2008. AnkyrinG is required for maintenance of the axon initial segment and neuronal polarity. J Cell Biol. 183:635–640.
Hotulainen P, Lappalainen P. 2006. Stress fibers are generated by two distinct actin assembly mechanisms in motile cells. J Cell Biol. 173:383–394.
Hund TJ, Koval OM, Li J, Wright PJ, Qian L, Snyder JS, Gudmundsson H, Kline CF, Davidson NP, Cardona N, et al. 2010. A beta(IV)-spectrin/CaMKII signaling complex is essential for membrane excitability in mice. J Clin Invest. 120:3508–3519.
Inda MC, DeFelipe J, Munoz A. 2006. Voltage-gated ion channels in the axon initial segment of human cortical pyramidal cells and their relationship with chandelier cells. Proc Natl Acad Sci U S A. 103:2920–2925.
Jedlicka P, Vlachos A, Schwarzacher SW, Deller T. 2008. A role for the spine apparatus in LTP and spatial learning. Behav Brain Res. 192:12–19.
Jenkins SM, Bennett V. 2001. Ankyrin-G coordinates assembly of the spectrin-based membrane skeleton, voltage-gated sodium channels, and L1 CAMs at Purkinje neuron initial segments. J Cell Biol. 155:739–746.
Jones EG, Powell TP. 1969. Synapses on the axon hillocks and initial segments of pyramidal cell axons in the cerebral cortex. J Cell Sci. 5:495–507.
Kole MH, Ilschner SU, Kampa BM, Williams SR, Ruben PC, Stuart GJ. 2008. Action potential generation requires a high sodium channel density in the axon initial segment. Nat Neurosci. 11:178–186.
Kosaka T. 1980. The axon initial segment as a synaptic site: ultrastructure and synaptology of the initial segment of the pyramidal cell in the rat hippocampus (CA3 region). J Neurocytol. 9:861–882.
Kremerskothen J, Plaas C, Kindler S, Frotscher M, Barnekow A. 2005. Synaptopodin, a molecule involved in the formation of the dendritic spine apparatus, is a dual actin/alpha-actinin binding protein. J Neurochem. 92:597–606.
Krupp JJ, Vissel B, Thomas CG, Heinemann SF, Westbrook GL. 1999. Interactions of calmodulin and alpha-actinin with the NR1 subunit modulate Ca^{2+}-dependent inactivation of NMDA receptors. J Neurosci. 19:1165–1178.
Kuba H, Oichi Y, Ohmori H. 2010. Presynaptic activity regulates Na(+) channel distribution at the axon initial segment. Nature. 465:1075–1078.
Kubota Y, Shigematsu N, Karube F, Sekigawa A, Kato S, Yamaguchi N, Hirai Y, Morishima M, Kawaguchi Y. 2011. Selective coexpression of multiple chemical markers defines discrete populations of neocortical GABAergic neurons. Cereb Cortex. 21:1803–1817.
Lek M, Quinlan KG, North KN. 2010. The evolution of skeletal muscle performance: gene duplication and divergence of human sarcomeric alpha-actinins. Bioessays. 32:17–25.
Linnemann A, van der Ven PF, Vakeel P, Albinus B, Simonis D, Bendas G, Schenk JA, Micheel B, Kley RA, Furst DO. 2010. The sarcomeric Z-disc component myopodin is a multiadapter protein that interacts with filamin and alpha-actinin. Eur J Cell Biol. 89:681–692.
Lorincz A, Nusser Z. 2008. Cell-type-dependent molecular composition of the axon initial segment. J Neurosci. 28:14329–14340.
Lu L, Timofeyev V, Li N, Rafizadeh S, Singapuri A, Harris TR, Chiamvimonvat N. 2009. Alpha-actinin2 cytoskeletal protein is required for the functional membrane localization of a Ca2+-activated K+ channel (SK2 channel). Proc Natl Acad Sci U S A. 106:18402–18407.
Mishra S, Chander V, Banerjee P, Oh JG, Lifirsu E, Park WJ, Kim do H, Bandyopadhyay A. 2011. Interaction of annexin A6 with alpha actinin in cardiomyocytes. BMC Cell Biol. 12:7.
Mundel P, Heid HW, Mundel TM, Kruger M, Reiser J, Kriz W. 1997. Synaptopodin: an actin-associated protein in telencephalic dendrites and renal podocytes. J Cell Biol. 139:193–204.
Nakagawa T, Engler JA, Sheng M. 2004. The dynamic turnover and functional roles of alpha-actinin in dendritic spines. Neuropharmacology. 47:734–745.
Okubo-Suzuki R, Okada D, Sekiguchi M, Inokuchi K. 2008. Synaptopodin maintains the neural activity-dependent enlargement of dendritic spines in hippocampal neurons. Mol Cell Neurosci. 38:266–276.
Otey CA, Carpen O. 2004. Alpha-actinin revisited: a fresh look at an old player. Cell Motil Cytoskeleton. 58:104–111.
Palay SL, Sotelo C, Peters A, Orkand PM. 1968. The axon hillock and the initial segment. J Cell Biol. 38:193–201.
Pascual J, Castresana J, Saraste M. 1997. Evolution of the spectrin repeat. Bioessays. 19:811–817.
Pelletier O, Pokidysheva E, Hirst LS, Bouxsein N, Li Y, Safinya CR. 2003. Structure of actin cross-linked with alpha-actinin: a network of bundles. Phys Rev Lett. 91:148102.
Peters A, Palay SL, Webster H, editors. 1991. The fine structure of the nervous system. 3rd ed. New York: Oxford University Press.
Peters A, Proskauer CC, Kaiserman-Abramof IR. 1968. The small pyramidal neuron of the rat cerebral cortex. The axon hillock and initial segment. J Cell Biol. 39:604–619.
Price CJ, Cauli B, Kovacs ER, Kulik A, Lambolez B, Shigemoto R, Capogna M. 2005. Neurogliaform neurons form a novel inhibitory network in the hippocampal CA1 area. J Neurosci. 25:6775–6786.
Rao A, Kim E, Sheng M, Craig AM. 1998. Heterogeneity in the molecular composition of excitatory postsynaptic sites during development of hippocampal neurons in culture. J Neurosci. 18:1217–1229.
Rasband MN. 2010. The axon initial segment and the maintenance of neuronal polarity. Nat Rev Neurosci. 11:552–562.
Ratzliff AD, Soltesz I. 2001. Differential immunoreactivity for alpha-actinin-2, an N-methyl-D-aspartate-receptor/actin binding protein, in hippocampal interneurons. Neuroscience. 103:337–349.
Rycroft BK, Gibb AJ. 2004. Regulation of single NMDA receptor channel activity by alpha-actinin and calmodulin in rat hippocampal granule cells. J Physiol. 557:795–808.
Sanchez-Ponce D, Munoz A, Garrido JJ. 2011a. Casein kinase 2 and microtubules control axon initial segment formation. Mol Cell Neurosci. 46:222–234.
Sanchez-Ponce D, Defelipe J, Garrido JJ, Munoz A. 2011b. In vitro maturation of the cisternal organelle in the hippocampal neuron's axon initial segment. Mol Cell Neurosci. 48:104–116.
Sanchez-Ponce D, Tapia M, Munoz A, Garrido JJ. 2008. New role of IKK alpha/beta phosphorylated I kappa B alpha in axon outgrowth and axon initial segment development. Mol Cell Neurosci. 37:832–844.
Schafer DP, Jha S, Liu F, Akella T, McCullough LD, Rasband MN. 2009. Disruption of the axon initial segment cytoskeleton is a new mechanism for neuronal injury. J Neurosci. 29:13242–13254.
Schroeter MM, Beall B, Heid HW, Chalovich JM. 2008. In vitro characterization of native mammalian smooth-muscle protein synaptopodin 2. Biosci Rep. 28:195–203.
Sloper JJ, Powell TP. 1979. A study of the axon initial segment and proximal axon of neurons in the primate motor and somatic sensory cortices. Philos Trans R Soc Lond B Biol Sci. 285:173–197.
Sobotzik JM, Sie JM, Politi C, Del Turco D, Bennett V, Deller T, Schultz C. 2009. AnkyrinG is required to maintain axo-dendritic polarity in vivo. Proc Natl Acad Sci U S A. 106:17564–17569.
Somogyi P, Nunzi MG, Gorio A, Smith AD. 1983. A new type of specific interneuron in the monkey hippocampus forming synapses exclusively with the axon initial segments of pyramidal cells. Brain Res. 259:137–142.

Stuart G, Schiller J, Sakmann B. 1997. Action potential initiation and propagation in rat neocortical pyramidal neurons. J Physiol. 505:617–632.

Tapia M, Wandosell F, Garrido JJ. 2010. Impaired function of HDAC6 slows down axonal growth and interferes with axon initial segment development. PLoS One. 5(9):e12908.

Vlachos A, Korkotian E, Schonfeld E, Copanaki E, Deller T, Segal M. 2009. Synaptopodin regulates plasticity of dendritic spines in hippocampal neurons. J Neurosci. 29:1017–1033.

Wachsstock DH, Schwartz WH, Pollard TD. 1993. Affinity of alpha-actinin for actin determines the structure and mechanical properties of actin filament gels. Biophys J. 65:205–214.

Walikonis RS, Jensen ON, Mann M, Provance DW Jr, Mercer JA, Kennedy MB. 2000. Identification of proteins in the postsynaptic density fraction by mass spectrometry. J Neurosci. 20: 4069–4080.

Walikonis RS, Oguni A, Khorosheva EM, Jeng CJ, Asuncion FJ, Kennedy MB. 2001. Densin-180 forms a ternary complex with the (alpha)-subunit of Ca2+/calmodulin-dependent protein kinase II and (alpha)-actinin. J Neurosci. 21:423–433.

Wang Y, Mattson MP, Furukawa K. 2002. Endoplasmic reticulum calcium release is modulated by actin polymerization. J Neurochem. 82:945–952.

Weins A, Schwarz K, Faul C, Barisoni L, Linke WA, Mundel P. 2001. Differentiation- and stress-dependent nuclear cytoplasmic redistribution of myopodin, a novel actin-bundling protein. J Cell Biol. 155:393–404.

Winckler B, Forscher P, Mellman I. 1999. A diffusion barrier maintains distribution of membrane proteins in polarized neurons. Nature. 397:698–701.

Wyszynski M, Kharazia V, Shanghvi R, Rao A, Beggs AH, Craig AM, Weinberg R, Sheng M. 1998. Differential regional expression and ultrastructural localization of alpha-actinin-2, a putative NMDA receptor-anchoring protein, in rat brain. J Neurosci. 18:1383–1392.

Wyszynski M, Lin J, Rao A, Nigh E, Beggs AH, Craig AM, Sheng M. 1997. Competitive binding of alpha-actinin and calmodulin to the NMDA receptor. Nature. 385:439–442.

Yamatani H, Kawasaki T, Mita S, Inagaki N, Hirata T. 2010. Proteomics analysis of the temporal changes in axonal proteins during maturation. Dev Neurobiol. 70:523–537.

Yu Y, Maureira C, Liu X, McCormick D. 2010. P/Q and N channels control baseline and spike-triggered calcium levels in neocortical axons and synaptic boutons. J Neurosci. 30:11858–11869.

Yu Y, Shu Y, McCormick DA. 2008. Cortical action potential back-propagation explains spike threshold variability and rapid-onset kinetics. J Neurosci. 28:7260–7272.

Zhang S, Ehlers MD, Bernhardt JP, Su CT, Huganir RL. 1998. Calmodulin mediates calcium-dependent inactivation of N-methyl-D-aspartate receptors. Neuron. 21:443–453.

Zhou D, Lambert S, Malen PL, Carpenter S, Boland LM, Bennett V. 1998. AnkyrinG is required for clustering of voltage-gated Na channels at axon initial segments and for normal action potential firing. J Cell Biol. 143:1295–1304.